JCTC Journal of Chemical Theory and Computation

First Principles Study of Alkali−Tyrosine Complexes: Alkali Solvation and Redox Properties

Francesca Costanzo,*,† Marialore Sulpizi,‡ Raffaele Guido Della Valle,† and Michiel Sprik‡

Dipartimento di Chimica Fisica e Inorganica and INSTM-UdR Bologna, Universita di Bologna, Viale Risorgimento 4, I-40136 Bologna, Italy, and, Department of Chemistry, University of Cambridge, Lensfield Road, CB2 1EW Cambridge, U.K.

Received February 6, 2008

Abstract: The oxidation of alkali-tyrosinate to radical alkali−tyrosine in aqueous solution is studied using ab initio Car−Parrinello molecular dynamics (CPMD). The aim is to investigate the cation-π interactions between alkali cations M and the aromatic ring of tyrosine, in gas phase and in aqueous solution, using the influence of the cation M on the reaction $M^+(Tyr^-) \rightarrow M^+(Tyr^*) + e^-$ as a probe. To this end, we calculate the redox potential and the reorganization free energy using a CPMD-based method derived from the Marcus theory of electron transfer. We discuss the redox properties of Tyr, Na^+(Tyr), and K^+(Tyr), in reduced and oxidized states, by analyzing selected interatomic distances, coordination numbers, and charge populations. Our results confirm the known inversion in the relative stabilities of Na^+(Tyr) and K^+(Tyr) in going from gas phase to solution and point to a stronger cation-π affinity of K^+ in solution.

1. Introduction

Cation-π interactions[1] involving aromatic amino acids are now recognized as a type of noncovalent-binding forces important for structure and function of proteins. Cation-π interactions have been shown to stabilize protein geometries[1] and to facilitate molecular recognition[1,2] at protein−protein interfaces[3] and in biological receptors.[4–6] The π system is provided by the aromatic rings of Phe, Tyr, and Trp, while the cations come from the positively charged side chains of Lys, Arg, and His. Cation-π interactions between aromatic amino acids and alkali cations are of particular interest, because of their role in ion selectivity.[3] K^+ channels, for example, show a highly conserved Gly-Tyr-Gly sequence, which is thought to be essential for the K^+ selectivity.[7,8]

Resolving the physical chemical nature of cation-π interactions and characterizing their properties has become a very active field of research,[4,9] both experimental and theoretical. Theoretical work[10–16] has focused on small model systems, by analyzing in detail the electrostatic, charge transfer, polarization, and covalent contributions to the binding.[4,17–19] Experimental and theoretical (computational) studies agree that in vacuum alkali cations are strongly bound, with the binding affinity for benzene-like systems following the electrostatic rules ($Li^+ > Na^+ > K^+$). In water solution, a dramatic reordering occurs,[20] and the cation-π affinity follows the order $K^+ > Na^+ > Li^+$. This is the same sequence seen in voltage-gated K^+ channels.[21]

In this work we present Car−Parrinello molecular dynamics (CPMD) simulations of metal−tyrosine complexes in water. The aim is to clarify the effect of the solvent on the stability of the cation-π complex, by comparing the binding of Na^+ and K^+. The phenol-alkali ion motif is a most relevant and popular model system for cation-π interactions in proteins and has been the subject of several computational studies.[1,10,14,15] The focus of these and related computational work has been on the neutral protonated closed shell state of the aromatic group. However, two of the three aromatic amino acid π electron donors, namely Tyr and Trp, are also well-known redox active amino acid residues. In the oxidized deprotonated state, these residues can stabilize unpaired electrons in radical enzymes (see for example refs 22−24). In particular, the neutral tyrosine radical is essential to the catalytic activity of class I ribonucleotide reductase and

* Corresponding author phone: +39-051-2093710; e-mail: costanzo@ms.fci.unibo.it.

† Universita di Bologna.

‡ University of Cambridge.

10.1021/ct8000415 CCC: $40.75
Published on Web 05/27/2008

similarly plays a central role in the generation of O_2 by plants in photosystem II.[25] Tryptophan cation radicals are involved, for example, in cytochrome oxidase. The redox chemistry of Tyr and Trp has been studied using relatively simple model complexes in solution[26–28] as well as de novo designed proteins.[29–31]

The link to radical enzyme catalysis prompted us to view the tyrosine-alkali ion pair from an electrochemical perspective and use the aqueous redox reaction as a probe of the interaction with Na^+ and K^+. The tyrosine residue in our model system is therefore either the deprotonated (oxidized) neutral radical (tyrosil), which will be indicated by Tyr*, or its anionic reduced form indicated by Tyr^-. Anticipating our results, we can confirm that a stronger affinity for the K^+ (Tyr) complex in aqueous solution correlates with an increase of the redox potential, due to a stronger stabilization of reduced K^+ (Tyr^-). While our study is limited to a single amino acid residue in solution, in an attempt to include some rudimentary aspects of the protein structure, we also discuss the role of the Tyr backbone in terms of both electrostatic and steric effects.

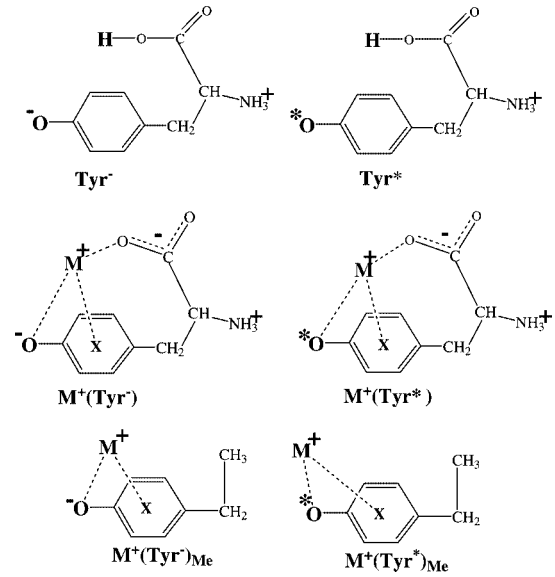

Figure 1. Structures of the reduced (left) and oxidized (right) states of tyrosine (top) and alkali cation-tyrosine complexes (middle). In the $M^+(Tyr^-)_{Me}$ structures (bottom), the zwitterionic backbone $-CH(NH_3^+)-COO^-$ is replaced by methyl $-CH_3$.

2. Methods

2.1. Model Complexes. As explained in the Introduction, we will use the redox properties of aqueous alkali cation complexes to probe the cation affinity of tyrosine in aqueous solution. The following three redox half-reactions will be compared

$$Tyr^- \rightarrow Tyr^* + e^- \quad (1)$$

$$Na^+(Tyr^-) \rightarrow Na^+(Tyr^*) + e^- \quad (2)$$

$$K^+(Tyr^-) \rightarrow K^+(Tyr^*) + e^- \quad (3)$$

We have first investigated the structural properties of the various molecular species, in vacuum and in aqueous solution, and then computed the redox potentials of each reaction. The species involved, shown in Figure 1, are the reduced (anionic) or oxidized (radical) states of deprotonated tyrosine, i.e. the acid phenolic proton is missing in all our model systems. While formally a tyrosyl, these species will also be referred to as tyrosine in the discussion below and indicated by the symbol Tyr. The metal-tyrosine (tyrosyl) complexes, either in reduced $M^+(Tyr^-)$ state or in oxidized $M^+(Tyr^*)$ state, are in zwitterionic form, since water solvation stabilizes the charge separation in the terminal groups $-NH_3^+$ and $-COO^-$. The metal M is either Na or K. For plain tyrosine (tyrosine without metal) we have chosen the form in which the carboxyl group is protonated. The charge of reduced Tyr^- or oxidized Tyr* is thus the same (0 or +1, respectively) as for the corresponding metal−tyrosine complexes (this is also a technical requirement in our redox free energy calculation scheme, see section 2.4). In the complexes labeled $M^+(Tyr^-)_{Me}$ and $M^+(Tyr^*)_{Me}$ (bottom of Figure 1) we have replaced the zwitterionic backbone $-CH(NH_3^+)-COO^-$ with a methyl group $-CH_3$. By comparison with the unsubstituted complexes, we obtain information on the importance of the backbone.

2.2. Electronic Structure Calculation. Calculations were performed with the CPMD package.[32] This is a general ab initio Car−Parrinello molecular dynamics code,[33] based on density functional theory. The BLYP functional[34,35] was used in all calculations. Only valence electrons were treated explicitly, and interactions with the ionic cores were described by norm-conserving pseudopotentials generated following the prescription by Troullier and Martins.[36] For Na^+ and K^+ the formal partition in valence and core is ambiguous because ionization eliminates the 3*s* respectively 4*s* valence electron. For this reason, the states 2*s* and 2*p* (for Na^+) and 3*s* and 3*p* (for K^+) in the next inner shell were treated as semicore states, effectively including them in the valence (for more details see for example the discussion in ref 37). The Kleinman-Bylander[38] decomposition was used for all the atomic species, with *s* and *p* nonlocality (angular momentum dependence) for C, N, O, and Na atoms. H atoms are represented by a simple *s* type pseudopotential. For consistency with the calculations in aqueous solution, described below in section 2.3, we chose a cubic cell with sides of 12.426 Å. Isolated system conditions were used in the gas-phase calculations. The Kohn−Sham orbitals were expanded in plane waves up to an energy cutoff of 70 Ry, which is sufficient to yield converged structural properties for water.[39] Only the Γ point was considered in the Brillouin zone integration. With regard to the accuracy of binding energy calculation in the gas phase, we further note that the use of a plane wave basis set, while computationally expensive, has the advantage that basis set superposition errors can in practice be neglected.

2.3. Molecular Dynamics Simulation. The systems in aqueous solution were equilibrated by preliminary classical MD simulations using the ORAC program.[40] These simulations were run at a constant number of particles, volume and temperature (NVT ensemble), using a Nose-Hoover thermostat at 300 K. A cubic cell with periodic boundary conditions and sides of 12.426 Å was adopted. The space not occupied by the $M^+(Tyr)$ solute was filled with SPC

water[41,42] with the experimental density at 300 K. The chosen box size, which requires 50 water molecules, allows space for at least one and a half layers of water around the M^+(Tyr) complex (whose largest dimension is ≈8.15 Å). Following the AMBER protocol,[43] the atomic charges for the solute were fitted to the ab initio electrostatic potential (ESP) evaluated with Gaussian03[44] at the B3LYP/6−31G* level.[34,35]

CPMD simulations were started using the classical equilibrated systems as the initial configuration. The time step was 5 au (about 0.12 fs). A fictitious electronic mass of 800 au was used to maintain the system on the Born−Oppenheimer surface. To reduce a possible bias of the initial classical configurations on the CPMD simulation, about 2 ps of equilibration with a Nose thermostat[45] at 300 K were followed by ≈8 ps of production run without temperature control (NVE ensemble).

2.4. Redox Properties Calculations. Redox properties for the reactions 1−3 were calculated using a MD method based on Marcus theory,[46] originally proposed by Warshel.[47] In the CPMD implementation applied here,[48–52] reaction free energies and reorganization energies of half-reactions are obtained from the vertical ionization energy gaps in the linear response approximation. Here we just recall the equations employed in the calculations. From the simulations of the systems in the oxidized states Na^+(Tyr*), K^+(Tyr*), or Tyr* and in the reduced states Na^+(Tyr$^-$), K^+(Tyr$^-$), or Tyr $^-$, the free energy of reduction (redox potential) ΔA and the reorganization free energy λ for the oxidation reactions 1−3 are computed from ensemble averages of the vertical ionization energy ΔE, as $\Delta A = (\langle\Delta E\rangle_O + \langle\Delta E\rangle_R)/2$ and $\lambda = (\langle\Delta E\rangle_R - \langle\Delta E\rangle_O)/2$. $\langle\Delta E\rangle_O$ denotes the average of the vertical ionization energies, as obtained from MD trajectories on the potential energy surface of the oxidized state O. $\langle\Delta E\rangle_R$ is the corresponding quantity on the surface of the reduced state R. The variance of the energy describes the fluctuations of the energy gap and is also of interest. There are again two such quantities, one for the reduced state $\sigma_R^2 = \langle(\Delta E - \langle\Delta E\rangle_R)^2\rangle_R$ and one for the oxidized state $\sigma_O^2 = \langle(\Delta E - \langle\Delta E\rangle_O)^2\rangle_O$. In the linear approximation employed here, the variance is independent of the oxidation state, $\sigma_R^2 = \sigma_O^2 = 2K_BT\lambda$. In practice this relation is used to verify whether the linear approximation is valid for a specific system.

The ΔA and λ estimates are computed directly from the vertical energies for removal of electrons from (or addition to) the periodic MD systems and are therefore subject to substantial finite size errors. These errors largely cancel when half-reaction energies are combined to yield reaction free energies of full redox reactions, provided that the charges of reactant and product species are the same (isoCoulombic reaction), that all calculations are carried out in MD cell of the same fixed length L, and that the redox active species are of similar size.[53] These conditions are satisfied for the reactions 1−3, and comparison of the computed half-reaction (oxidation) free energies is therefore meaningful. Moreover, as argued in ref 53 on the basis of a periodic continuum model and demonstrated for a classical model system, the finite size correction for ΔA scales with the inverse volume ($1/L^3$) of the MD cell rather than inverse length ($1/L$). This is a result of screening by the solvent with high dielectric constant (water). Experience with the (limited) set of reactions investigated so far indicates that full reaction free energies agree with experiment within a margin of about 0.2 eV (for a recent compilation see ref 54). Unfortunately, the full $1/L$ long-range effect is recovered for the reorganization energy λ which, as a result, is seriously underestimated (in the order of one eV) in the small samples used here.[53]

Table 1. Binding Energies (kcal/mol) of the Metal−Tyrosine Complexes in the Gas Phase and Distances r (Å) from the Cation M to X_π, O_{Ph}, and O_{carb}[a]

system	binding energy	$r_{M\text{-}X_\pi}$	$r_{M\text{-}O_{Ph}}$	$r_{M\text{-}O_{carb}}$
Na^+(Tyr$^-$)	−152.22	3.07	2.29	2.18
Na^+(Tyr*)	−62.83	3.45	2.51	2.22
K^+(Tyr$^-$)	−133.09	3.30	2.68	2.58
K^+(Tyr*)	−49.32	3.90	2.80	2.58
Na^+(Tyr$^-$)$_{Me}$	−129.70	3.65	2.13	
Na^+(Tyr*)$_{Me}$	−40.29	4.76	2.14	
K^+(Tyr$^-$)$_{Me}$	−112.00	4.01	2.39	
K^+(Tyr*)$_{Me}$	−27.12	4.86	2.63	

[a] Center of phenolic ring and phenolic and carboxylic oxygens.

3. Results and Discussion

3.1. M^+(Tyr) Complexes in Gas Phase. Since gas-phase plain tyrosine is already well studied,[10,14] and, moreover, it is not stable in zwitterionic form, we have studied only the metal−tyrosine complexes (see Figure 1). The vertical binding energy of the various complexes and the distances from the cation M to X_π, O_{Ph}, and O_{carb} (center of phenolic ring, phenolic, and carboxylic oxygens, respectively) are shown in Table 1. The binding energies are calculated for the optimized geometry of the complex, as the optimized geometry of the complex, as $E_{M^+(Tyr)} - E_{M^+} - E_{Tyr}$. All E_{Tyr} energies are calculated with all atoms kept in the geometry of the complex and thus do not include the deformation energy required to bring the uncomplexed neutral molecule into its complexed geometry. The reduced complexes Na^+(Tyr$^-$) and K^+(Tyr$^-$) are significantly lower in energy than their oxidized counterparts, due to the increased Coulomb attraction between the negatively charged O_{Ph} and the positively charged metals. The $r_{M\text{-}O_{Ph}}$ and $r_{M\text{-}X_\pi}$ distances are also smaller in the reduced state. Comparing now the results for the two alkali cations, we see that the binding energy for Na^+(Tyr$^-$) is about 20 kcal/mol stronger than for K^+(Tyr$^-$). In the oxidized forms the binding energy difference between Na^+ and K^+ decreases to 14 kcal/mol, with the Na^+ complex remaining the most stable. This decreased stabilization might be related to a bending of about 20° observed for the phenyl ring in Na^+(Tyr*). For the M^+(Tyr) complexes containing neutral (protonated) tyrosine the published results[10,14] point in the same direction. There are no M-O_{Ph} interactions in these systems, and the difference between Na^+(Tyr) and K^+(Tyr) further decreases to 13 kcal/mol.

To quantify the contribution of the backbone to the binding with the metal, we have considered the $M^+(Tyr)_{Me}$ complex (Figure 1) in which the zwitterionic backbone -CH(NH_3^+)-COO^- is replaced by a methyl group -CH_3. The overall effect of removing the backbone is that the metal moves slightly away from the π-ring and comes closer to O_{Ph} (Table 1),

Table 2. Simulation Averages for $Na^+(Tyr^-)$, $Na^+(Tyr^*)$, $K^+(Tyr^-)$, $K^+(Tyr^*)$, Tyr^-, and Tyr^* in Aqueous Solution[a]

system	$r_{M\text{-}X_\pi}$	$r_{M\text{-}O_{Ph}}$	$r_{M\text{-}O_{carb}}$	$n_{M\text{-}Ow}$	$n_{O_{Ph}\text{-}Hw}$	$Q_{Mulliken}$	$Q_{Löwdin}$
$Na^+(Tyr^-)$	4.4 ± 0.4	5.6 ± 0.4	2.7 ± 0.6	3.95	3.14	−0.30 ± 0.02	−0.24 ± 0.02
$Na^+(Tyr^*)$	4.7 ± 1.0	6.1 ± 1.1	2.6 ± 0.5	3.90	2.60	−0.23 ± 0.01	−0.16 ± 0.01
$K^+(Tyr^-)$	3.6 ± 0.4	4.1 ± 0.4	3.2 ± 0.5	3.87	3.40	−0.31 ± 0.01	−0.25 ± 0.02
$K^+(Tyr^*)$	4.7 ± 0.6	5.5 ± 1.0	3.1 ± 0.6	4.19	2.24	−0.20 ± 0.02	−0.14 ± 0.02
Tyr^-	3.8 ± 0.2	5.2 ± 0.3		1.00	3.16	−0.30 ± 0.02	−0.25 ± 0.03
Tyr^*	3.9 ± 0.3	5.3 ± 0.4		1.00	2.46	−0.22 ± 0.01	−0.15 ± 0.01

[a] The table reports the distances r (Å) from the cation M to X_π, O_{Ph}, and O_{carb} (center of phenolic ring and phenolic and carboxylic oxygens), the coordination numbers $n_{M\text{-}Ow}$ and $n_{OPh\text{-}Hw}$ (where Ow or Hw indicate water oxygens or hydrogens), and the Mulliken and Löwdin charges Q for O_{Ph}. In the absence of alkali metal, the carboxylic hydrogen H_{carb} takes the role of the cation M. Standard deviations are given where appropriate.

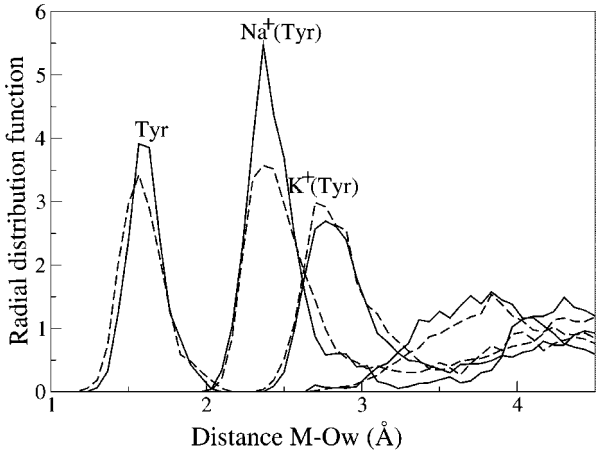

Figure 2. Radial distribution function $g_{M\text{-}Ow(r)}$ between the cation M and the water oxygens Ow for $Na^+(Tyr)$, $K^+(Tyr)$, and Tyr, as indicated. For Tyr, M corresponds to H_{carb}. Solid and dashed lines represent reduced and oxidized systems, respectively.

thus optimizing the electrostatics in the absence of $M\text{-}O_{carb}$ interactions. The zwitterionic backbone is responsible for an energy stabilization of ≈22 kcal/mol for all structures, leaving unchanged the stability order $Na^+(Tyr^-) > K^+(Tyr^-) > Na^+(Tyr^*) > K^+(Tyr^*)$. In view of the importance of the $-CH(NH_3^+)-COO^-$ backbone in the gas phase, we have included it in all the following simulations in aqueous solution. Presence of the backbone is a possibly significant difference with the only available CPMD simulation of a cation-π interaction in water, which is for a solvated ammonium−benzene complex.[16]

3.2. Cation Coordination in Aqueous Solution. All complexes shown in Figure 1 (namely $Na^+(Tyr^-)$, $Na^+(Tyr^*)$, $K^+(Tyr^-)$, $K^+(Tyr^*)$, Tyr^-, and Tyr^*) were investigated in aqueous solution by carrying out independent MD runs (for setting see section 2.3). The structural analysis will focus on the interactions between the cation M and its environment and on the effect of the redox induced change of charge of the phenolic oxygen O_{Ph}. In Table 2 we report a selection of relevant CPMD averages, which includes interatomic distances r and coordination numbers n around M or O_{Ph} and estimates of the charge Q on O_{Ph}. In Figure 2 we display the radial distribution function $g_{M\text{-}Ow(r)}$ between the cation M and the water oxygens Ow. For plain tyrosine, in the absence of metal, the carboxylic hydrogen H_{carb} takes the role of the cation M.

The $Na^+(Tyr^-)$ and $Na^+(Tyr^*)$ complexes have similar $g_{M\text{-}Ow(r)}$ peak shapes (Figure 2), coordination numbers $n_{Na\text{-}Ow}$, and distances $r_{Na\text{-}X_\pi}$ and $r_{Na\text{-}O_{Ph}}$ (Table 2). The oxidation state of tyrosine evidently has only very little influence on the solvation of Na^+. The effect is more pronounced for the $K^+(Tyr)$ complex. Even though the $g_{M\text{-}Ow(r)}$ peak shapes (Figure 2) appear quite similar in the reduced and the oxidized states, the contraction of $r_{K\text{-}X_\pi}$ and $r_{K\text{-}O_{Ph}}$ upon reduction is larger for the K^+ complex (≈1 Å for K^+ compared to ≈0.5 Å for Na^+, see Table 2). Moreover, while the difference in coordination number $n_{K\text{-}Ow}$ for $K^+(Tyr^-)$ relative to $K^+(Tyr^*)$ is not very large (≈0.3), this decrease is significant in comparison to the Na^+ complex, for which coordination remains essentially unchanged in the redox reaction. We should mention here that the coordination numbers $n_{M\text{-}Ow}$ have been obtained by integrating $g_{M\text{-}Ow(r)}$ up to the first minimum, identified at $r_0 = 3.4$ and 3.5 Å for Na and K, respectively. The dependence of $n_{M\text{-}Ow}$ on the chosen cutoff r_0 is not a cause of concern, since the differences among the various $n_{M\text{-}Ow}$ are, within reasonable ranges, largely independent of r_0.

We interpret these results on coordination as evidence that reduction enhances the electrostatic interaction of K^+ with the π aromatic electrons and the O_{Ph} oxygen, whereas the effect for Na^+ is relatively unimportant. This suggests that the affinity of K^+ toward the π system is stronger compared to Na^+. This behavior is opposite to that for the affinity in the gas phase, where both distances and binding energies indicate that the complexes with Na^+ are more stable than the complexes with K^+. Our finding is in agreement with the reordering in solution predicted by Kumpf and Dougherty[21] and indicates that this reordering is still present in the deprotonated tyrosine and is not affected by its oxidation state.

Qualitative differences between aqueous Na^+ and K^+ are well-known. Aqueous solutions of these cations, even when of equal ionic strength, can have strikingly different effects on biopolymers, notably on folding and aggregation of proteins (Hofmeister effect, for a recent review see ref 55). These issues have attracted renewed attention in the recent literature. The explanation is generally sought in short-range effects such as the stability of the first hydration shell. A crucial feature distinguishing the two ions, according to this line of thought, is that Na^+ tends to hold onto its first solvation shell in inhomogeneous environments, while it is easier for K^+ to give up some of its coordinated water molecules in exchange for direct interactions with other

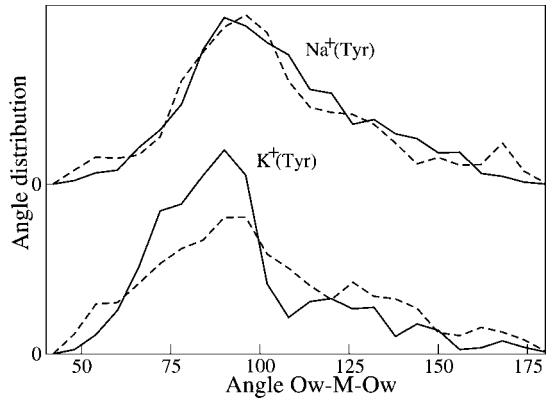

Figure 3. Ow-M-Ow bond angle distributions for Na^+(Tyr) and K^+(Tyr), as indicated. Solid and dashed lines represent reduced and oxidized systems, respectively.

species. Such a mechanism may also play a role in our system. This conjecture is supported by a comparison of the water coordination for our alkali ion-tyrosine complexes to the coordination in bulk solution. CPMD calculations on alkali cations[37,56–58] give for these ions fully solvated in water coordination numbers $n_{Na\text{-}Ow} = 5.2$ and $n_{K\text{-}Ow} = 7.1$. By comparison with our results for $M^+(Tyr^-)$ and $M^+(Tyr^*)$, we find that the cation-π interaction displaces about 1.3 water molecules in the case of Na^+ and 3.0 molecules for K^+. Further confirmation comes from the anisotropy of the hydration of the cations in the complex with tyrosine. We determined the angular distributions of the water molecules around Na^+ and K^+ by averaging over our MD trajectories. Figure 3 shows the distribution of the Ow-M-Ow angles formed by the metal and two water oxygens. For Na^+(Tyr) the angular distributions in the reduced and oxidized states have similar shape and angle range. For K^+(Tyr) the reduced form exhibits a sharper peak in the range $75-100^{\circ}$. This finding correlates with the shorter $r_{M\text{-}X_\pi}$. Since the K^+ is closer than Na^+ to the π ring, it has less space to coordinate water molecules.

Finally, we investigate plain tyrosine for a possible OH-π interaction involving the carboxyl hydrogen H_{carb}. This investigation is motivated by the examples, found in proteins, of configurations in which the OH side chain of an amino acid is arranged face-on to the aromatic face of a tyrosine.[59] For plain tyrosine, indeed, Table 2 indicates relatively short distances $r_{M\text{-}X_\pi}$ (where M correspond to H_{carb}). This may confirm a OH-π interaction between the H_{carb} proton and the ring. For both Tyr^- and Tyr^*, we have noticed that H_{carb} is interacting with one water molecule only ($n_{M\text{-}Ow} = 1$) over the entire simulation.

3.3. Solvation of the Phenoxyl Oxygen. We now turn to the solvation of O_{Ph}, which is directly involved in the redox process. We find (Table 2) that the coordination numbers $n_{O_{Ph}\text{-}Hw}$ for the various complexes strongly correlate with the electrostatic charges on O_{Ph} (linear correlation coefficient $r \geq 0.98$, for both Mulliken and Löwdin). For both metals, the coordination number $n_{O_{Ph}\text{-}Hw}$ increases in going from the oxidized to the reduced complexes, due to the enhanced electrostatic interactions of the water hydrogens with the larger charge residing on the O_{Ph}. The K^+ complexes show the largest change in coordination numbers $n_{O_{Ph}\text{-}Hw}$ (1.16 versus 0.54 for the Na^+ complex). The changes in the charge of O_{Ph} are less pronounced (−0.11 for K^+ compared to −0.07 for Na^+, according to the data of Table 2). We note that for the K^+ complex the response of $n_{O_{Ph}\text{-}Hw}$ to reduction is opposite to that of $n_{K\text{-}Ow}$, discussed in section 3.2. While $n_{K\text{-}Ow}$ decreases, $n_{O_{Ph}\text{-}Hw}$ increases. There is no such a clear (anti) correlation for the Na^+ complex, consistently with our picture of a stronger reduction induced ion pairing for K^+ compared to Na^+.

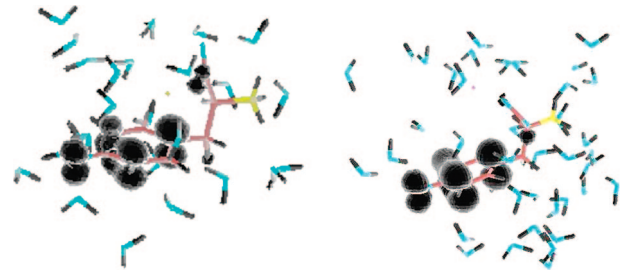

Figure 4. Unpaired spin density for $Na^+(Tyr^*)$ (left) and $K^+(Tyr^*)$ (right). The isosurface represents the spin density at 0.005 e au^{-3}.

Table 3. Averages $\langle \Delta E \rangle_R$ and $\langle \Delta E \rangle_O$ of the Vertical Transition Energies (eV) for the Reduced and Oxidized States, Respectively[a]

system	$\langle \Delta E \rangle_R$	$\langle \Delta E \rangle_O$	ΔA	λ
Na^+(Tyr)	1.25 ± 0.20	−0.11 ± 0.24	0.57 ± 0.16	0.68 ± 0.16
K^+(Tyr)	1.36 ± 0.19	−0.05 ± 0.19	0.66 ± 0.13	0.70 ± 0.13
Tyr	1.32 ± 0.20	0.00 ± 0.22	0.66 ± 0.15	0.66 ± 0.15

[a] Helmholtz free energy of reduction ΔA, reorganization energy λ, and all standard deviations σ are also reported.

The unpaired spin density for the oxidized systems $K^+(Tyr^*)$ and $Na^+(Tyr^*)$ is shown in Figure 4. The spin density is mostly localized on the O_{Ph}, C_{ortho}, and C_{para} positions around the phenoxyl ring, in agreement with previous calculations.[60] As expected for Na^+ and K^+ bound to the aromatic ring, even in aqueous solution, the unpaired spin density on the metal is negligible, supporting the known picture where electrostatics plays a predictive role in cation-π interactions.[19]

3.4. Redox Free Energies. The vertical ionization energies ΔE for the various reduced and oxidized systems in aqueous solution, calculated as described in section 2.4, are shown in Table 3. The table also reports the resulting free energies of reduction ΔA, the reorganization free energies λ, and all standard deviations σ. The agreement between the variances of the vertical ionization energies in the oxidized and the reduced state is sufficient to justify the use of the linear response approximation for the estimation of ΔA and λ (see section 2.4). The free energy change ΔA, in the definition used here, is the Helmholtz free energy of reduction. It is therefore tempting to interpret the positive sign of ΔA as evidence that the reduced forms of the cation−tyrosine complex are more stable than the oxidized forms. This would be consistent with the behavior of the distances, coordination numbers, and charges, discussed in the previous sections. Indeed, the stabilizing effect of the cation-π interaction on the reduced form (increasing the

redox potential ΔA) has already been noticed by NMR experiments on tryptophan.[29–31]

Unfortunately, as repeatedly pointed out in earlier works,[48–51,53,54] using a similar half-reaction scheme, the utmost caution is required when interpreting half-reaction energies. Finite size effects in our small periodic systems can seriously bias energies if the net charge of the MD cell is changed. In ref 53 it was shown that the interactions with periodic images of the redox active species and the neutralizing homogeneous background charge artificially stabilize the species with the higher charge. This effect can even invert the sign the oxidation free energy ΔA. However, the reduced state, which is the state favored by our calculated half-reaction free energies for the cation−tyrosine complexes, has net charge zero. It is the oxidized state, the state with the higher free energy, which is charged. This observation, specific to our system, gives us some confidence that the sign of ΔA can be, after all, regarded as an indication that the reduced species with the anionic phenoxyl ring is the more stable, although the actual numerical value is not reliable for the reasons explained.

Of special interest in the present context are the relative values of ΔA in Table 3, which are far less sensitive to finite size effects. The differences in ΔA are in the 50−100 meV range. These values are comparable to the standard deviations of ΔA, indicated in Table 3, which are all around 150 meV. The statistical errors on the averages, which are computed over $N = 130$ configurations sampled from a time window of at least 5 ps, can therefore be assumed to be substantially smaller. A reasonable estimate of the uncertainty, obtained by taking into account[61] the statistical correlations between consecutive configurations, is 20 meV. The relative difference in ΔA of 90 meV between K^+ and Na^+, although small, therefore appears to be statistically significant. The difference is in the expected direction and confirms that K^+ interacts more strongly with the π aromatic electrons of tyrosine consistent with the analysis of the complex geometries of section 3.2. Finally, K^+(Tyr) and Tyr are found to have similar redox potentials ΔA (Table 3), suggesting that comparable strong cation-π interactions also occur for plain tyrosine, with the carboxylic hydrogen H_{carb} playing a role similar to K^+, as also indicated by the short $r_{M\text{-}X_\pi}$ distances (Table 3).

The reorganization energy λ, which is not experimentally accessible, describes the response of the solvent to the change of the charge distribution on the complex as a result of the oxidation process. The calculated reorganization energies λ are similar for all the species studied. A likely explanation is that the relaxation is dominated by an outer-sphere process, which is approximately the same for these closely related systems.

4. Conclusions

Using Car−Parrinello molecular dynamics (CPMD), we have investigated the cation-π interactions between Na^+ or K^+ alkali cations and the aromatic ring of tyrosine, in gas phase and in aqueous solution. The binding energy difference in gas phase and the free energy of reduction in solution (calculated within the Marcus theory of electron transfer) indicate that the reduced forms are, in all cases, more stable than the oxidized forms. This greater stability correlates with shorter distances $r_{M\text{-}X_\pi}$ and (in solution) with larger coordination numbers $n_{O_{Ph}\text{-}Hw}$ (where M, X_π, O_{Ph}, and Hw indicate alkali metal, center of phenolic ring, phenolic oxygen, and water hydrogens, respectively). Thus, we deduce that the cation-π interaction stabilizes the reduced forms of both metal−tyrosine complexes. A further observation is that in the absence of a metal ion, the carboxylic hydrogen H_{carb} can take over the role of the cation M.

The influence of the coordination by alkali cations (either Na^+ or K^+) on the reaction $M^+(Tyr^-) \rightarrow M^+(Tyr^*) + e^-$ is rather intriguing. In gas phase, in agreement with the literature[10,14] our calculations show the Na^+(Tyr) complexes to be more stable in both reduced and oxidized states, independently of any additional stabilization due to the zwitterionic backbone. A reordering of the cation affinities occurs in solution, again in agreement with literature.[11,21,62] Analysis of simulation observables shows the K^+ cation is partly desolvated in the reduced state, while Na^+ largely keeps its first solvation shell. The shorter distance $r_{K\text{-}X_\pi}$, the smaller coordination $n_{M\text{-}Ow}$, the enhanced hydrogen bonding of O_{Ph}, and the sharper Ow-M-Ow angular distribution, all show the K^+ to be more involved in the interaction with the π aromatic electrons.

The structural analysis has been backed up by a free energy calculation. Failing a full and, at the ab initio MD level, exceedingly expensive determination of the dissociation constant from a potential of mean force for the attraction between alkali atoms and the tyrosine ring, we have used the redox properties of the equilibrium complex as a probe of the energetics. We have found a difference of 90 meV between the redox potentials of K^+ and Na^+, with the reduced state of the K^+ forming the most stable complex (Table 3). This free energy difference is just above the lower margin of what can be considered statistically significant in our CPMD simulation scheme. Retrospectively, we could have expected such a difficulty, since energy increments important on the "bioscale" are typically in the order of one pK unit (60 meV). The experimental difference between the redox potentials of tyrosine and tryptophan, for example, is 110 meV.[63] This is at the limit of the current CPMD methods, with yield accuracies around 100 meV.[54]

The overall picture emerging from our calculations is that in solution K^+ has stronger cation-π interactions than Na^+. This is supported by our CPMD results for the distance and coordination observables and is consistent with our results for the redox properties. Our calculations therefore confirm experimental[62] and other theoretical[21] studies arriving at a similar conclusion. This result is important in the biological field, where the difference between the two alkali metals is fundamental in physiological processes related to the K channels, such as electrical signaling in the nervous system, regulation of cardiac excitability and regulation of insuline release.[8]

Acknowledgment. Work done with funds from MIUR (PRIN project and FIRB project through INSTM consortium). We warmly thank M. Boero for providing the pseudopotentials, P. Procacci for support with the ORAC

program, Prof. Brillante for useful discussions, and the EPCC Supercomputer Center for an allocation of computer resources within the HPC-Europa program.

References

(1) Dougherty, D. A. Cation-π Interactions in Chemistry and Biology: A New View of Benzene, Phe, Tyr, and Trp. *Science* **1996**, *271*, 163–168.

(2) Dougherty, D. A.; Stauffer, D. A. Acetylcholine Binding by a Synthetic Receptor. Implications for Biological Recognition. *Science* **1990**, *250*, 1558–1560.

(3) Cabarcos, O. M.; Weinheimer, C. J.; Lisy, J. M. Size selectivity by cation-π interactions: Solvation of K^+ and Na^+ by benzene and water. *J. Chem. Phys.* **1999**, *110*, 8429–8435.

(4) Ma, J. C.; Dougherty, D. A. The Cation-π Interaction. *Chem. Rev.* **1997**, *97*, 1303–1324.

(5) Brejc, K.; van Dijk, W. J.; Klaassen, R. V.; Schuurmans, M.; van der Oost, J.; Smit, A. B.; Sixma, T. K. The crystal structure of AChBP, homolog of the N-terminal domain of the nicotinic acetylcholine receptor. *Nature* **2001**, *411*, 269–276.

(6) Gromiha, M. M.; Santhosh, C.; Ahmad, S. Structural analysis of cation-π interactions in DNA binding proteins. *Int. J. Biol. Macromol.* **2004**, *34*, 203–211.

(7) Heginbotham, L.; MacKinnon, R. The aromatic binding site for tetraethylammonium ion on potassium channels. *Neuron* **1992**, *8*, 483–491.

(8) Domene, C.; Sansom, M. S. P. Potassium channel, ions, and water: simulation studies based on the high resolution X-ray structure of KcsA. *Biophys. J.* **2003**, *85*, 2787–2800.

(9) Meyer, E. A.; Castellano, R. K.; Diederich, F. Interactions with Aromatic Rings in Chemical and Biological Recognition. *Angew. Chem. Int. Ed.* **2003**, *42*, 1210–1250.

(10) Dunbar, R. C. Complexation of Na^+ and K^+ to Aromatic Amino Acids: A Density Functional Computational Study of Cation-π Interactions. *J. Phys. Chem. A* **2000**, *104*, 8067–8074.

(11) Ryzhov, V.; Dunbar, R. C.; Cerda, B.; Wesdemiotis, C. Cation-π Effects in the Complexation of Na^+ and K^+ with Phe, Tyr, and Trp in the Gas Phase. *J. Am. Soc. Mass. Spectrom.* **2000**, *11*, 1037–1046.

(12) Siu, F. M.; Ma, N. L.; Tsang, C. W. Cation-π Interactions in Sodiated Phenylalanine Complexes: Is Phenylalanine in the Charge-Solvated or Zwitterionic Form? *J. Am. Chem. Soc.* **2001**, *123*, 3397–3398.

(13) Gapeev, A.; Dunbar, R. C. Na^+ affinities of gas-phase amino acids by ligand exchange equilibrium. *Int. J. Mass. Spectrom.* **2003**, *228*, 825–839.

(14) Ruan, C.; Rodgers, M. T. Cation-π Interactions: Structure and Energetics of Complexation of Na^+ and K^+ with the Aromatic Amino Acids, Phenylalanine, Tyrosine, and Tryptophan. *J. Am. Chem. Soc.* **2004**, *126*, 14600–14610.

(15) Reddy, A. S.; Sastry, G. N. Cation [M = H^+, Li^+, Na^+, K^+, Ca^{2+}, Mg^{2+}, NH_4^+, and NMe_4^+] Interactions with the Aromatic Motifs of Naturally Occurring Amino Acids: A Theoretical Study. *J. Phys. Chem. A* **2005**, *109*, 8893–8903.

(16) Sa, R.; Zhu, W.; Shen, J.; Gong, Z.; Cheng, J.; Chen, K.; Jiang, H. How Does Ammonium Dynamically Interact with Benzene in Aqueous Media? A First Principle Study Using the Car-Parrinello Molecular Dynamics Method. *J. Phys. Chem. B* **2006**, *110*, 5094–5098.

(17) Costanzo, F.; Della Valle, R. G.; Barone, V. MD simulation of the Na^+-phenylalanine complex in water: competition between cation-π interaction and aqueous solvation. *J. Phys. Chem. B* **2005**, *109*, 23016–23023.

(18) Cubero, E.; Luque, F. J.; Orozco, M. Is polarization important in cation-π interactions? *Proc. Natl. Acad. Sci.* **1998**, *95*, 5976–5980.

(19) Mecozzi, S.; West, A. P.; Dougherty, D. A. Cation-π Interactions in Simple Aromatics: Electrostatics Provide a Predictive Tool. *J. Am. Chem. Soc.* **1996**, *118*, 2307–2308.

(20) Hu, J.; Barbour, L. J.; Gokel, G. W. Probing alkali metal-π interactions with the side chain residue of tryptophan. *Proc. Natl. Acad. Sci*. **2002,** *99*, 5121−5126.

(21) Kumpf, R. A.; Dougherty, D. A. A Mechanism for Ion Selectivity in Potassium Channels: Computational Studies of Cation-π Interactions. *Science* **1993**, *261*, 1708–1710.

(22) Stubbe, J.; van der Donk, W. A. Protein Radicals in Enzyme Catalysis. *Chem. Rev.* **1998**, *98*, 705–762.

(23) Stubbe, J. Radicals with a controlled lifestyle. *Chem. Commun.* **2003**, *20*, 2511–2513.

(24) Himo, F.; Siegbahn, P. E. M. Quantum Chemical Studies of Radical-Containing Enzymes. *Chem. Rev.* **2003**, *103*, 2421–2456.

(25) Ishikita, H.; Knapp, E.-W. Function of Redox-Active Tyrosine in Photosystem II. *Biophys. J.* **2006**, *90*, 3886–3896.

(26) Sjödin, M.; Styring, S.; Åkermark, B.; Sun, L. Hammarström, L. Proton-coupled electron transfer from tyrosine in a tyrosine-ruthenium-tris-bipyridine complex: Comparison with $Tyrosine_z$ oxidation in photosystem II. *J. Am. Chem. Soc.* **2000**, *122*, 3932–3936.

(27) Sjödin, M.; Styring, S.; Wolpher, H.; Xu, Y.; Sun, L.; Hammarström, L. Switching the Redox Mechanism: Models for Proton-Coupled Electron Transfer from Tyrosine and Tryptophan. *J. Am. Chem. Soc.* **2005**, *127*, 3855–3863.

(28) Carra, C.; Iordanova, N.; Hammegs-Schiffer, S. Proton-Coupled Electron Transfer in a Model for Tyrosine Oxidation in Photosystem II. *J. Am. Chem. Soc.* **2003**, *125*, 10429–10436.

(29) Tommos, C.; Skalicky, J. J.; Pilloud, D. L.; Wand, A. J.; Dutton, P. L. De novo proteins as models of radical enzymes. *Biochemistry* **1999**, *38*, 9495–9507.

(30) Dai, Q.-H.; Tommos, C.; Fuentes, E. J.; Blomberg, M. R. A.; Dutton, P. L.; Wand, A. J. Structure of a de Novo Designed Protein Model of Radical Enzymes. *J. Am. Chem. Soc.* **2002**, *124*, 10952–10953.

(31) Westerlund, K.; Berry, B. W.; Privett, H. K.; Tommos, C. Exploring amino-acid radical chemistry: protein engineering and de novo design. *Biochim. Biophys. Acta* **2005**, *1707*, 103–116.

(32) CPMD version 3.11, Copyright IBM Corp 1990−2006, Copyright MPI für Festkrperforschung Stuttgart 1997−2001. http://www.cpmd.org/ (accessed March 7, 2008).

(33) Car, R.; Parrinello, M. Unified Approach for Molecular Dynamics and Density-Functional Theory. *Phys. Rev. Lett.* **1985**, *55*, 2471–2474.

(34) Becke, A. D. Density-functional exchange-energy approximation with correct asymptotic behavior. *Phys. Rev. A* **1988**, *38*, 3098–3100.

(35) Lee, C.; Yang, W.; Parr, R. G. Development of the Colle-Salvetti correlation-energy formula into a functional of the electron density. *Phys. Rev. B* **1988**, *37*, 785–789.

(36) Troullier, N.; Martins, J. L. Efficient pseudopotentials for plane-wave calculations. *Phys. Rev. B* **1991**, *43*, 1993–2006.

(37) Vuilleumier, R.; Sprik, M. Electronic properties of hard and soft ions in solution: Aqueous Na^+ and Ag^+ compared. *J. Chem. Phys.* **2001**, *115*, 3454–3468.

(38) Kleinman, L.; Bylander, D. M. Efficacious Form for Model Pseudopotentials. *Phys. Rev. Lett.* **1982**, *48*, 1425–1428.

(39) VandeVondele, J.; Mohamed, F.; Krack, M.; Hutter, J.; Sprik, M.; Parrinello, M. The influence of temperature and density functional models in ab initio molecular dynamics simulation of liquid water. *J. Chem. Phys.* **2005**, *122*, 014515/1–6.

(40) Procacci, P.; Darden, T. A.; Paci, E.; Marchi, M. ORAC: A Molecular Dynamics Program to Simulate Complex Molecular Systems with Realistic Electrostatic Interactions. *J. Comput. Chem.* **1997**, *18*, 1848–1862. http://www.chim.unifi.it/orac/ (accessed March 7, 2008)

(41) Berendsen, H. J. C.; Grigera, J. R.; Straatsma, T. P. The Missing Term in Effective Pair Potential. *J. Phys. Chem.* **1987**, *91*, 6269–6271.

(42) Straatsma, T. P.; Berendsen, H. J. C. Free energy of ionic hydration: Analysis of a thermodynamic integration technique to evaluate free energy differences by molecular dynamics simulations. *J. Chem. Phys.* **1988**, *89*, 5876–5886.

(43) Cornell, W. D.; Cieplak, P.; Bayly, C. I.; Gould, I. R.; Merz, K. M., Jr.; Ferguson, D. M.; Spellmeyer, D. C.; Fox, T.; Caldwell, J. W.; Kollman, P. A. A Second Generation Force Field for the Simulation of Proteins, Nucleic Acids, and Organic Molecules. *J. Am. Chem. Soc.* **1995**, *117*, 5179–5197.

(44) Frisch, M. J.; Trucks, G. W.; Schlegel, H. B.; Scuseria, G. E.; Robb, M. A.; Cheeseman, J. R.; Montgomery, J. A., Jr.; Vreven T.; Kudin, K. N.; Burant, J. C.; Millam, J. M.; Iyengar, S. S.; Tomasi, J.; Barone, V.; Mennucci, B.; Cossi, M.; Scalmani, G.; Rega, N.; Petersson, G. A.; Nakatsuji, H.; Hada, M.; Ehara, M.; Toyota, K.; Fukuda, R.; Hasegawa, J.; Ishida, M.; Nakajima, T.; Honda, Y.; Kitao, O.; Nakai, H.; Klene, M.; X. Li, Knox, J. E.; Hratchian, H. P.; Cross, J. B.; Adamo, C.; Jaramillo, J.; Gomperts, R.; Stratmann, R. E.; Yazyev, O.; Austin, A. J.; Cammi, R.; Pomelli, C.; Ochterski, J. W.; Ayala, P. Y.; Morokuma, K.; Voth, G. A.; Salvador, P; Dannenberg, J. J.; Zakrzewski, V. G., Dapprich, S.; Daniels, A. D.; Strain, M. C.; Farkas, O., Malick, D. K.; Rabuck, A. D., Raghavachari, K.; Foresman, J. B.; Ortiz, J. V., Cui, Q.; Baboul, A. G.; Clifford, S.; Cioslowski, J.; Stefanov, B. B.; Liu, G.; Liashenko, A.; Piskorz, P.; Komaromi, I., Martin, R. L., Fox, D. J., Keith, T., Al-Laham, M. A.; Peng, C. Y.; Nanayakkara, A.; Challacombe, M.; Gill, P. M. W.; Johnson, B., Chen, W., Wong, M. W.; Gonzalez., C.; Pople, J. A. *Gaussian 03, Revision B.05*; Gaussian, Inc.: Pittsburgh, PA, 2003.

(45) Nose, S. A unified formulation of the constant temperature molecular dynamics methods. *J. Chem. Phys.* **1984**, *81*, 511–519.

(46) Marcus, R. A.; Sutin, N. Electron transfers in chemistry and biology. *Biochim. Biophys. Acta* **1985**, *811*, 265–322.

(47) Warshel, A. Dynamics of Reactions in Polar Solvents. Semiclassical Trajectory Studies of Electron Transfer and Proton Transfer Reactions. *J. Phys. Chem.* **1982**, *86*, 2218–2224.

(48) Tateyama, Y.; Blumberger, J.; Sprik, M.; Tavernelli, I. Density-functional molecular-dynamics study of the redox reactions of two anionic, aqueous transition-metal complexes. *J. Chem. Phys.* **2005**, *122*, 234505/1–17.

(49) Blumberger, J.; Sprik, M. Quantum versus classical electron transfer energy as reaction coordinate for the aqueous Ru^{+2} /Ru^{+3} redox reaction. *Theor. Chem. Acc.* **2006**, *115*, 113–126.

(50) Blumberger, J.; Tavernelli, I.; Klein, M.; Sprik, M. Diabatic free energy curves and coordination fluctuations for the aqueous Ag^+ /Ag^{+2} redox couple: A biased Born-Oppenheimer molecular dynamics investigation. *J. Chem. Phys.* **2006**, *124*, 064507/1–12.

(51) VandeVondele, J.; Sulpizi, M.; Sprik, M. From Solvent Fluctuations to Quantitative Redox Properties of Quinones in Methanol and Acetonitrile. *Angew. Chem., Int. Ed.* **2006**, *45*, 1936–1938.

(52) Sulpizi, M.; Raugei, S.; VandeVondele, J.; Carloni, P.; Sprik, M. Calculation of Redox Properties: Understanding Short- and Long-Range Effects in Rubredoxin. *J. Phys. Chem. B* **2007**, *111*, 3969–3976.

(53) Ayala, R.; Sprik, M. A Classical Point Charge Model Study of System Size Dependence of Oxidation and Reorganization Free Energies in Aqueous Solution. *J. Phys. Chem. B* **2008**, *112*, 257–269.

(54) VandeVondele, J.; Ayala, R.; Sulpizi, M.; Sprik, M. Redox free energies and one-electron energy levels in density functional theory based ab initio molecular dynamics. *J. Electroanal. Chem.* **2007**, *607*, 113–120.

(55) Collins, K. D.; Neilson, G. W.; Enderby, J. E. Ions in water: Characterizing the forces that control chemical processes and biological structure. *Biophys. Chem.* **2007**, *128*, 95–104.

(56) Ramaniah, L. M.; Bernasconi, M.; Parrinello, M. Ab initio molecular-dynamics simulation of K^+ solvation in water. *J. Chem. Phys.* **1999**, *111*, 1587–1591.

(57) White, J. A.; Schwegler, E.; Galli, G.; Gygi, F. The solvation of Na^+ in water: First-principles simulations. *J. Chem. Phys.* **2000**, *113*, 4668–4673.

(58) Ikeda, T.; Boero, M.; Terakura, K. Hydration of alkali ions from first principles molecular dynamics revisited. *J. Chem. Phys.* **2007**, *126*, 034501/1–9.

(59) Sulpizi, M.; Carloni, P. Cation-π versus OH- π Interactions in Proteins: A Density Functional Study. *J. Phys. Chem. B* **2000**, *104*, 10087–10091.

(60) Wu, P.; O'Malley, P. J. Environmental effects on phenoxyl free radical spin densities and hyperfine couplings. *J. Mol. Struct. THEOCHEM* **2005**, *730*, 251–254.

(61) Allen, M. P.; Tildesley, D. J. How to analyse the results. In *Computer Simulation of Liquids*; Oxford University Press Inc.: New York, 1987; Section 6.4, pp 191−195.

(62) Zhu, D.; Herbert, B. E.; Schlautman, M. A.; Carraway, E. R. Characterization of Cation-π Interactions in Aqueous Solution Using Deuterium NMR Spectroscopy. *J. Environ. Qual.* **2004**, *33*, 276–284.

(63) DeFelippis, M. R.; Murthy, C. P.; Faraggi, M.; Klapper, M. H. Pulse Radiolytic Measurement of Redox Potentials: The Tyrosine and Tryptophan Radicals. *Biochemistry* **1989**, *28*, 4847–4853.

CT8000415